Effects of Ligand and Solvent on the Synthesis of Iron Oxide Nanoparticles from $Fe(acac)_3$ Solution by Femtosecond Laser Irradiation

Takuya Okamoto, Takahiro Nakamura, Yuhei O. Tahara, Makoto Miyata, Kenji Sakota, Tomoyuki Yatsuhashi

Effects of Ligand and Solvent on the Synthesis of Iron Oxide Nanoparticles from $Fe(acac)_3$ Solution by Femtosecond Laser Irradiation

Takuya Okamoto,[1] Takahiro Nakamura,[2] Yuhei O. Tahara,[1] Makoto Miyata,[1] Kenji Sakota,[1] and Tomoyuki. Yatsuhashi*[1]
[1] *Graduate School of Science, Osaka City University, 3-3-138 Sugimoto, Sumiyoshi-ku, Osaka 558–8585 Japan*
[2] *Institute of Multidisciplinary Research for Advanced Materials, Tohoku University, 2-1-1 Katahira, Aoba-ku, Sendai 980-857 Japan*

E-mail: tomo@sci.osaka-cu.ac.jp

Synthesis of iron oxide nanoparticles (Fe-O NPs) from iron(III)acetylacetonate solution by femtosecond laser irradiation is reported. Fe-O NPs and carbon are agglomerated in *n*-hexane, while single-nanometer-sized dispersed Fe-O NPs are obtained in water. We propose that the choice of ligands and solvent determines the primary particle size distribution and dispersion states of NPs as well as carbon contaminants in laser-assisted synthesis using metal complexes as reactants.

Keywords: Solvent | Metal complex | Size distribution

Nanoparticles (NPs) have specific chemical and physical properties that are size-dependent and differ from the properties of their bulk form.[1] Many synthetic methods have been proposed, such as chemical synthesis methods like co-precipitation,[2] solvothermal treatment,[3] and thermal decomposition.[4] In the past decade, the syntheses of NPs in liquid by using pulsed lasers have attracted much attention by virtue of their simplicity. Laser-assisted NP syntheses in liquid can be classified into three approaches. First, pulsed laser ablation in liquid, in which bulk materials are ablated in an inert solvent, is a representative top-down approach.[5] Second, bottom-up syntheses of noble metal (Au, Ag, Pt, etc.) NPs from metal ion solution by femtosecond laser irradiation have been reported.[6] The reactive species (e_{aq}^-, $H^\bullet$, etc.) generated by multiphoton ionization of water molecules[7] can reduce metal ions followed by the aggregation of metal atoms to form metal NPs. However, the reduction of base metal ions (e.g., Fe^{2+}) is difficult because the reduction of such metal ions to metal atoms is an endothermic process.[8] It is emphasized that iron oxide nanoparticles (Fe-O NPs) have been regarded as promising materials applicable to bio-imaging,[9] drug delivery,[10] hyperthermia,[11] and so on. In order to synthesize Fe-O NPs, we can apply a third method: photochemical reaction of a metal complex solution, which is another bottom-up approach. Ferrocene ($Fe(C_5H_5)_2$),[12-14] $Fe(CO)_5$,[15] iron(II)acetylacetonate ($Fe(C_5H_7O_2)_2$),[16] and iron(III)acetylacetonate ($Fe(C_5H_7O_2)_3$)[17] have been used as reactants. In most cases, Fe-O NPs were covered with carbon materials.[12,13,15,16] Recently, we reported the synthesis of carbon shell-free Fe-O NPs, but the particles were larger than 20 nm.[14] This made them unsuitable for biocompatible[18] and superparamagnetic[19] Fe-O NPs, which must be smaller than 20 nm for medical applications such as hyperthermia.[20]

In this study, we report the synthesis of single-nanometer-sized Fe-O NPs from iron(III)acetylacetonate solution by femtosecond laser irradiation. The morphologies, primary particle size distributions, elemental mappings, and crystal structures are compared for Fe-O NPs obtained in different solvents such as *n*-hexane and water. The effects of ligands and solvents on the carbon products and the size and dispersion states of Fe-O NPs are discussed.

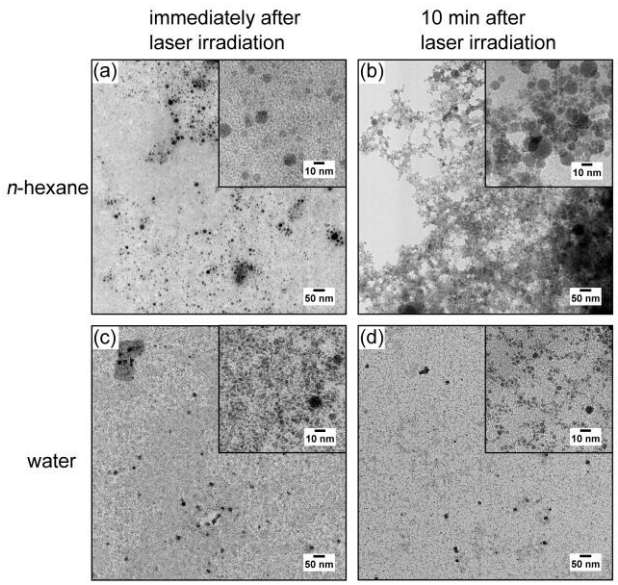

Figure 1. TEM images of Fe-O NPs obtained in (a, b) *n*-hexane and (c, d) water after the 25-min laser irradiation (scale bar: 50 nm; inset, 10 nm) . Colloidal solution was dropped onto a TEM grid (a, c) immediately or (b, d) 10 min after laser irradiation.

Iron(III)acetylacetonate ($Fe(acac)_3$, Nacalai Tesque, ≥95.0%), *n*-hexane (Nacalai Tesque, ≥96.0%), and distilled water (Nacalai Tesque) were used without further purification. The concentration of $Fe(acac)_3$ in *n*-hexane or water was 1.0×10^{-3} mol dm^{-3}. Femtosecond laser pulses (0.8 μm, 40 fs, 0.4 mJ, 1 kHz) were focused on the $Fe(acac)_3$ solution in a quartz cuvette with a 1-cm optical path length by using a planoconvex lens with a focal length of 50 mm. Details of the laser experiments have been described elsewhere.[21] The laser irradiation was performed under air atmosphere at 296 K. Fe-O NPs were observed by using a transmission electron microscope (TEM, JEM-1010, JEOL) operated at an acceleration voltage of 80 kV. For the preparation of specimens for TEM observations, 10 μL of sample solution was directly dropped onto a copper grid covered with an amorphous carbon film (Nisshin EM) followed by drying in an air at room temperature. The primary particle size distributions of Fe-O NPs were analyzed by using image processing software (ImageJ 1.48 v) provided by National Institutes of Health. Elemental

mapping using an energy-dispersive X-ray spectrometer (EDS), high-angle annular dark field scanning TEM (HAADF-STEM), and high-resolution TEM (HR-TEM) measurements were performed by using Titan G2 Cubed (FEI) operated at 300 kV. In these measurements, a copper grid covered with amorphous silicon film (Okenshoji) was used as a substrate to avoid carbon contaminants during observation.

Figure 1 shows TEM images of Fe-O NPs obtained in *n*-hexane or water after the 25-min laser irradiation. We prepared these specimens by dropping colloidal solution immediately or 10 min after the laser irradiation. In the former cases, dispersed Fe-O NPs smaller than 10 nm in diameter were observed regardless of solvent (Figure 1a, c). In the latter cases, the agglomerates of net-like carbons and Fe-O NPs were observed for the sample collected from *n*-hexane (Figure 1b), whereas dispersed Fe-O NPs (<10 nm) were obtained for the sample collected from water (Figure 1d). The pH of water did not change by 25-min femtosecond laser irradiation. These findings indicate that the dispersion state of colloidal solution changes after the laser irradiation and post-laser reaction proceeds, especially when *n*-hexane is used as a solvent. The mean sizes of the Fe-O NPs collected immediately after the 25-min laser irradiation were 10.5±3.5 (*n*-hexane) and 4.9±1.9 nm (water), respectively (Figures 2 and S1). Those collected 10-min after the 25-min laser irradiation were 12.9±5.3 (*n*-hexane) and 4.9±1.7 nm (water), respectively (Figure S1). Figure 2 shows the primary particle size distributions of Fe-O NPs collected immediately after the laser irradiation. The peak of the primary particle size distributions of the Fe-O NPs obtained in *n*-hexane gradually increased as the duration of laser irradiation increased. In contrast, the peak of the primary particle size distribution of the Fe-O NPs obtained in water was below 10 nm regardless of the laser irradiation time.

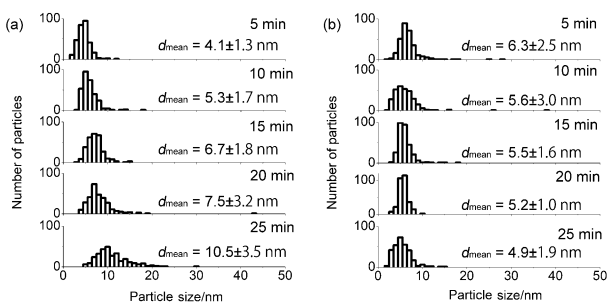

Figure 2. The primary particle size distributions of Fe-O NPs obtained in (a) *n*-hexane and (b) water. The sample was exposed to femtosecond laser pulses for the duration indicated on the upper right-hand corner of each graph. The sample was collected immediately after the laser irradiation. d_{mean} denotes the mean size. Batch-type experiments were carried out. Each sample contained 300 particles.

Figure 3 shows TEM images and elemental mappings of iron, carbon, and oxygen of the Fe-O NPs collected 10 min after the laser irradiation. We can identify two regions in the elemental mapping images. One is the region where iron overlapped with oxygen but without carbon, and the other is the region where iron, oxygen, and carbon overlapped. The former region, which is indicated by white dotted circles in the bright field images, was found in isolated Fe-O NPs obtained in *n*-hexane and in the highly agglomerated Fe-O NPs obtained in water. The other region in mapping images was shared by iron, carbon, and oxygen. These different regions can be clearly observed by the reconstructed images of iron and carbon distributions and HAADF-STEM images, and by the line scan analyses shown in Figure 4. As clearly shown in Figure 4a (obtained in *n*-hexane), the isolated particles (colored in green) did not contain carbon, whereas agglomerated regions (colored in yellow) were composed of iron and carbon. We conclude that this region is occupied by a mixture of Fe-O NPs and carbon particles. In contrast, the reconstructed image of Fe-O NPs obtained in water (Figure 4b) shows that the amount of carbon was negligible. Further, it is obvious that the locations of iron and carbon did not overlap. We conclude that carbon is not incorporated in Fe-O NPs synthesized in water.

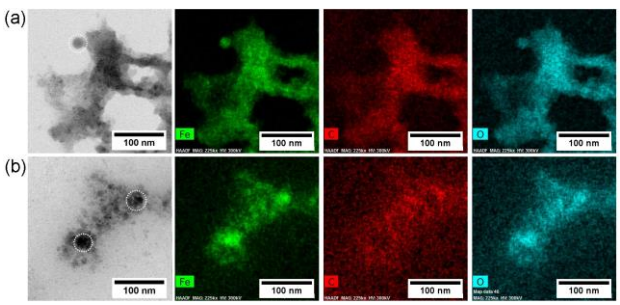

Figure 3. TEM images and elemental mappings of Fe-O NPs obtained in (a) *n*-hexane and (b) water after the 25-min laser irradiation (scale bar: 100 nm). The sample was collected 10 min after the laser irradiation.

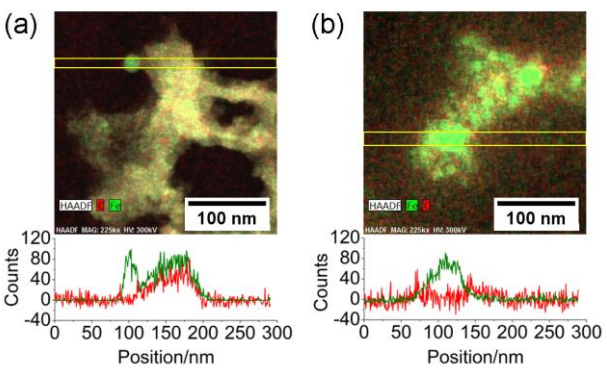

Figure 4. Elemental mapping of Fe-O NPs obtained in (a) *n*-hexane and (b) water after the 25-min laser irradiation (scale bar: 100 nm). (upper panels) Reconstructed images of iron and carbon distributions, and HAADF-STEM image. (lower panels) Elemental distributions obtained by EDS line scans. The scanned area is indicated by the yellow square frames shown in the upper panels. The sample was collected 10 min after the laser irradiation.

Figure 5 shows the HR-TEM images of Fe-O NPs collected 10 min after the 25-min laser irradiation. The interplanar spacings and assignments of crystal planes are shown. The lattice fringe patterns of observed for Fe-O NPs were in good agreement with the calculated values using the unit length of magnetite (Fe_3O_4: 8.3941 Å).[22] Based on the results obtained above, we identified most of the spherical Fe-O NPs as magnetite particles.

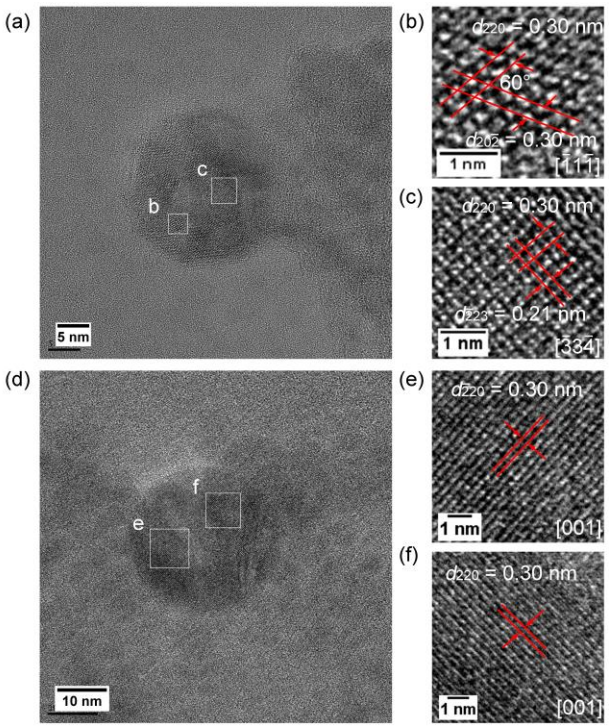

Figure 5. HR-TEM images of Fe-O NPs obtained in (a-c) *n*-hexane (scale bar: a, 5 nm; b and c, 1 nm) and (d-f) water after the 25-min laser irradiation (scale bar: d, 10 nm; e and f, 1 nm). Values in brackets denote the zone axes of electron beam incidence.

We expect that Fe-O NPs were formed by photochemical reactions as in the case of ferrocene in *n*-hexane solution.[14] Oxidation may occur by the reactive oxygen species formed in water or by dissolved oxygen in *n*-hexane (the concentrations of oxygen in *n*-hexane under air atmosphere is 3.1×10^{-3} mol dm^{-3}.)[23] We reported that carbon agglomerates are produced as contaminants originating from ligands in laser-assisted NP synthesis using ferrocene *n*-hexane solution.[14] The decreases in carbon agglomerates in the cases of $Fe(acac)_3$ compared with similar experiments using ferrocene as a reactant are attributable to the character of the ligands: cyclopentadienyl ligands form carbon agglomerates, whereas acetylacetonate ligands do not. This is understood by the analogy that carbon NPs emerge from aromatics but not from aliphatic hydrocarbons under laser irradiation conditions similar to those used in the present experiments.[21,24] In water, the source of carbon should be liberated ligands; however, the elemental mapping showed that the distributions of iron and carbon did not coincide with each other. In *n*-hexane, we did not observe carbon agglomerates or core-shell structures in Fe-O NPs for the sample collected immediately after the laser irradiation (Figure 1a), whereas net-like carbon agglomerates appeared 10 min after the laser irradiation (Figure 1b). Hu et al. reported that plenty of diamond-like carbons covering iron NPs were formed by femtosecond laser irradiation of an iron plate in *n*-hexane.[25] At present, we do not have a definitive conclusion about the appearance of the agglomerates of Fe-O NPs and carbons. We propose that carbonization promoted by the catalytic reaction of *n*-hexane on the surface of Fe-O NPs might play a role in the formation of net-like carbons, where agglomerated Fe-O NPs are captured.

We next consider the effect of ligands on the particle growth process during laser irradiation. The mean size of Fe-O NPs obtained from ferrocene *n*-hexane solution (1.0×10^{-3} mol dm^{-3}) was about 25 nm by the 25-min laser irradiation (Figure S1 in Ref. 14). Here we emphasize that the mean size of Fe-O NPs obtained from $Fe(acac)_3$ in *n*-hexane was about half that of those obtained in ferrocene *n*-hexane solution even though the experimental conditions (solvent, concentration, laser parameters) were the same. Moreover, the mean size of the Fe-O NPs that emerged from $Fe(acac)_3$ became ca. 5 nm by using water as a solvent. We propose that the ligands (acetylacetonate anions) of $Fe(acac)_3$ protect the particles from aggregation because of their strong coordination ability.[26] Even though acetylacetonate anions may not cover the whole particle surface, this effect is important for regulating the size of Fe-O NPs. Of course, laser fragmentation in liquid[5,14,27] might play a role in suppressing the particle growth.

This study demonstrates that the choice of ligands and solvents strongly affects the morphology, primary particle size distributions, and dispersion state of Fe-O NPs synthesized from iron complexes by femtosecond laser irradiation. Fe-O NPs with carbon shell have been obtained by the laser ablation of an iron plate in organic liquid regardless of laser irradiation paramaters,[28] and by photochemical reaction of metal complexes in aromatic solvent.[12,13,15] We suggest that the choice of reactants (metal complexes) and solvent (aliphatics) as well as pulse duration (femtosecond) and wavelength (near-infrared) of laser pulse is important to produce carbon shell-free metal NPs.[14] Furthermore, the use of $Fe(acac)_3$ decreases the mean size of Fe-O NPs down to the single-nanometer level, presumably because acetylacetonates prevent primary particles from growing by coordination. We suggest that metal complexes are not only a source of metal but also play an important role in determining nanoparticle structures in laser-assisted NP synthesis.

This work was supported in part by THE AMADA FOUNDATION Grant for Laser Processing Grant Number AF-2017224 for T. Y., JSPS KAKENHI Grant Number 18J15442 for T. O. This work was performed under the Research Program for Next Generation Young Scientists of "Five-star Alliance" in "NJRC Mater. & Dev" for T. O. and the Cooperative Research Program in "NJRC Mater. & Dev." for T. Y. We thank Mr. Yuichiro Hayasaka for his

help with EDS measurements. We thank Mr. Kazuhiko Kondo of Thales Japan Inc. for his kind contribution to our laser system.

Supporting Information is available on http://dx.doi.org/10.1246/cl.******.

References and Notes

1 R. Kubo, *J. Phys. Soc. Jpn.* **1962**, *17*, 975; M. A. El-Sayed, *Acc. Chem. Res.* **2001**, *34*, 257; E. Roduner, *Chem. Soc. Rev.* **2006**, *35*, 583.

2 T. Q. Bui, S. N.-C. Ton, A. T. Duong, H. T. Tran, *J. Sci. Adv. Mater. Devices* **2018**, *3*, 107.

3 N. Pinna, G. Garnweitner, M. Antonietti, M. Niederberger, *J. Am. Chem. Soc.* **2005**, *127*, 5608.

4 N. Jović Orsini, B. Babić-Stojić, V. Spasojević, M. P. Calatayud, N. Cvjetićanin, G. F. Goya, *J. Magn. Magn. Mater.* **2018**, *449*, 286.

5 D. Zhang, B. Gökce, S. Barcikowski, *Chem. Rev.* **2017**, *117*, 3990; D. Amansa, W. Cai, S. Barcikowski, *Appl. Surf. Sci*. **2019**, *488*, 445.

6 T. Nakamura, Y. Mochidzuki, S. Sato, *J. Mater. Res.* **2008**, *23*, 968; T. Nakamura, H. Magara, Y. Herbani, S. Sato, *Appl. Phys. A* **2011**, *104*, 1021; T. Nakamura, K. Takasaki, A. Ito, S. Sato, *Appl. Surf. Sci.* **2009**, *255*, 9630; N. Nakashima, K. Yamanaka, M. Saeki, H. Ohba, S. Taniguchi, T. Yatsuhashi, *J. Photochem. Photobiol. A* **2016**, *319*, 70; T. Okamoto, T. Nakamura, K. Sakota, T. Yatsuhashi, *Langmuir* **2019**, *35*, 12123.

7 S. L. Chin, S. Lagacé, *Appl. Opt.* **1996**, *35*, 907.

8 N. Nakashima, K. Yamanaka, A. Itoh, T. Yatsuhashi, *Chin. J. Phys.* **2014**, *52*, 504.

9 J. Gao, H. Gu, B. Xu, *Acc. Chem. Res.* **2009**, 42, 1097.

10 T. K. Jain, M. A. Morales, S. K. Sahoo, D. L. Leslie-Pelecky, V. Labhasetwar, *Mol. Pharm.* **2005**, 2, 194.

11 J.-P. Fortin, C. Wilhelm, J. Servais, C. Ménager, J.-C. Bacri, F. Gazeau, *J. Am. Chem. Soc.* **2007**, 129, 2628.

12 J. B. Park, S. H. Jeong, M. S. Jeong, J. Y. Kim, B. K. Cho, *Carbon* **2008**, *46*, 1369.

13 M. J. Wesolowski, S. Kuzmin, B. Wales, J. H. Sanderson, W. W. Duley, *J. Mater. Sci.* **2013**, *48*, 6212.

14 T. Okamoto, T. Nakamura, R. Kihara, T. Asahi, K. Sakota, T. Yatsuhashi, *ChemPhysChem* **2018**, *19*, 2480.

15 S. Moussa, G. Atkinson, M. S. El-Shall, *J. Nanoparticle Res.* **2013**, *15*, 1470.

16 J. Pola, M. Maryško, V. Vorlíček, S. Bakardjieva, J. Šubrt, Z. Bastl, A. Ouchi, *J. Photochem. Photobiol. A* **2008**, *199*, 156.

17 M. Watanabe, H. Takamura, H. Sugai, *Nanoscale Res. Lett.* **2009**, *4*, 565.

18 T. K. Jain, M. K. Reddy, M. A. Morales, D. L. Leslie-Pelecky, V Labhasetwar, *Mol. Pharm.* **2008**, 5, 316.

19 A.-H. Lu, E. L. Salabas, F. Schüth, *Angew. Chem. Int. Ed.* **2007**, *46*, 1222.

20 S. Sun, H. Zeng, *J. Am. Chem. Soc.* **2002**, *124*, 8204.

21 T. Hamaguchi, T. Okamoto, K. Mitamura, K. Matsukawa, T. Yatsuhashi, *Bull. Chem. Soc. Jpn.* **2015**, *88*, 251.

22 M. E. Fleet, *Acta Crystallogr. B* **1981**, *37*, 917.

23 *Handbook of Photochemistry*, 3rd. Ed., ed. by M. Montalti, A. Credi, L. Priodi, M. T. Gandolfi, CRC Press, NW, **2006**.

24 T. Okamoto, K. Mitamura, T. Hamaguchi, K. Matsukawa, T. Yatsuhashi, *ChemPhysChem* **2017**, *18*, 1007; T. Yatsuhashi, N. Uchida, K. Nishikawa, *Chem. Lett.* **2012**, *41*, 722.

25 A. Hu, J. Sanderson, Y. Zhou, W. W. Duley, *Diam. Relat. Mater.* **2009**, *18*, 999.

26 E. K. C. Pradeep, M. Ohtani, T. Kawaharamura, K. Kobiro, *Chem. Lett.* **2017**, *46*, 940.

27 L. Delfour, T. E. Itina, *J. Phys. Chem. C* **2015**, *119*, 13893.

28 V. Amendola, M. Meneghetti, *Phys. Chem. Chem. Phys.* **2013**, *15*, 3027.

Graphical Abstract

Textual Information

A brief abstract	The primary particle size distribution and dispersion state of iron oxide nanoparticles synthesized from iron(III)acetylacetonate by femtosecond laser irradiation depend strongly on the solvent used. Dispersed single-nanometer-size iron oxide nanoparticles are obtained in water, while iron oxide nanoparticles obtained in *n*-hexane are highly agglomerated with carbons after the laser irradiation presumably due to the catalytic carbonization.
Title	Effects of Ligand and Solvent on the Synthesis of Iron Oxide Nanoparticles from $Fe(acac)_3$ Solution by Femtosecond Laser Irradiation
Authors' Names	Takuya Okamoto, Takahiro Nakamura, Yuhei O. Tahara, Makoto Miyata, Kenji Sakota, Tomoyuki Yatsuhashi

Graphical Information